Poly(nonylbisoxazole): A Member of a New Class of Conjugated Polymer

Jeffrey K. Politis and M. David Curtis*

Department of Chemistry and the Macromolecular Science and Engineering Center, The University of Michigan, Ann Arbor, Michigan 48109-1055

L. González-Ronda and David C. Martin

Department of Materials Science and Engineering and the Macromolecular Science and Engineering Center, The University of Michigan, Ann Arbor, Michigan 48109-2136

Received May 8, 2000. Revised Manuscript Received June 26, 2000

The synthesis of poly(4,4′-dinonyl-2,2′-bisoxazole-5,5′-diyl) (PNBO) was performed through a nickel-mediated coupling of 5,5′-dibromo-4,4′-dinonyl-2,2′-bisoxazole. The solid-state morphology of PNBO was determined by powder X-ray diffraction (XRD) which showed strong peaks due to lamellar spacing and three-dimensional ordering. The polymer has absorbance maxima of 446 and 464 nm in solution, and 475 nm in the film. A low wavelength shoulder near 510 nm is ascribed to the absorption of aggregated molecules. The emission spectra are concentration dependent and consistent with emission from excimers. Essentially all the emission in the solid state is due to excimers. The physical and chemical properties of PNBO are compared to the sulfur analogues, poly(4,4′-dinonyl-2,2′-bithiazole-5,5′-diyl) (PNBTz) and poly(3-alkylthiophene)s.

Introduction

Tuning the properties of conjugated polymers is a focus of many research groups due to the different requirements needed to achieve good performance in various devices. However, it is difficult to alter a specific property while maintaining others constant. For example, the methods used in tuning the emission wavelength for light-emitting diodes (LEDs) are generally accompanied by changes in solid-state morphology and/or electrochemical behavior. The emission color is altered by three general methods: increasing steric congestion in the side chains,[1−4] the use of electron-withdrawing and electron-donating groups (EWG and EDG) directly bonded to the main chain, and copolymerization with nonconjugated segments. Bulky substituents force the rings to twist out of coplanarity and cause blue shifts in absorption and emission wavelengths. The twisting of the polymer backbone also disrupts the solid-state packing. EWGs or EDGs cause shifts in the emission wavelength by raising or lowering the energy levels of the HOMO and LUMO.[5−8] The energy levels of the HOMO and LUMO are directly related to the redox behavior of the polymer, and hence, the electrochemical potentials are also altered. The introduction of nonconjugated flexible segments blue shifts the emission λ_{max}, but also changes the solid-state ordering and transport properties.[9−17]

A much less studied approach toward altering polymer properties is the replacement of specific atoms along the polymer backbone. For example, replacing carbon with nitrogen in poly(*p*-phenylenevinylene) (PPV) leads to poly(pyridine vinylene) (PPyV).[18,19] The addition of the more electronegative nitrogen into the conjugated system increases (makes more positive) the reduction potential. Similarly, replacement of a ring C atom with a N atom in poly(3-alkythiophenes) (P3ATs) gives rise to poly(alkylbithiazoles) (PABTs) which have increased oxidation and reduction potentials vis-à-vis the P3ATs, but whose solid-state morphologies, thermochromism, etc., are very similar.[20−24]

(1) Inganas, O.; Berggren, M.; Andersson, M. R.; Gustafsson, G.; Hjertberg, T.; Wennerstrom, O.; Dyreklev, P.; Granstrom, M. *Synth. Met.* **1995**, *71*, 2121.
(2) Andersson, M. R.; Berggren, M.; Inganas, O.; Gustafsson, G.; Gustafsson-Carlberg, J. C.; Selse, D.; Hjertberg, T.; Wennerstrom, O. *Macromolecules* **1995**, *28*, 7525.
(3) Luzzati, S.; Prevosti, E.; Catellani, M. *Synth. Met.* **1997**, *84*, 551.
(4) Antoniadis, H.; Roitman, D.; Hsieh, B.; Feld, W. F. *Polym. Adv. Technol.* **1997**, *8*, 392.
(5) Doi, S.; Kuwabara, M.; Noguchi, T.; Ohnishi, T. *Synth. Met.* **1993**, *55−57*, 4174.
(6) Greenham, N. C.; Moratti, S. C.; Bradley, D. D. C.; Friend, R. H.; Holmes, A. B. *Nature* **1993**, *365*, 628.
(7) Gurge, R. M.; Sarker, A. M.; Lahti, P. M.; Hu, B.; Karasz, F. E. *Macromolecules* **1997**, *30*, 8286.
(8) Lux, A.; Holmes, A. B.; Cervini, R.; Davies, J. E.; Moratti, S. C.; Gruner, J.; Cacialli, F.; Friend, R. H. *Synth. Met.* **1997**, *84*, 293.
(9) Burn, P. L.; Holmes, A. B.; Kraft, A.; Bradley, D. D. C.; Brown, A. R.; Friend, R. H.; Gymer, R. W. *Nature* **1992**, *356*, 47.
(10) Burn, P. L.; Holmes, A. B.; Kraft, A.; Bradley, D. D. C.; Brown, A. R.; Friend, R. H. *J. Chem. Soc., Chem. Commun.* **1992**, 32.
(11) Kraft, A.; Burn, P. L.; Holmes, A. B. *Synth. Met.* **1993**, *55−57*, 936.
(12) Holmes, A. B.; Bradley, D. D. C.; Brown, A. R.; Burn, P. L.; Burroughes, J. H.; Friend, R. H.; Greenham, N. C.; Gymer, R. W.; Halliday, D. A.; Jackson, R. W.; Kraft, A.; Martens, J. H. F.; Pichler, K.; Samuel, I. D. W. *Synth. Met.* **1993**, *55−57*, 4031.
(13) Hu, B.; Karasz, F. E. *Synth. Met.* **1998**, *92*, 157.
(14) Hay, M.; Klavetter, F. L. *J. Am. Chem. Soc.* **1995**, *117*, 7112.
(15) Kim, H. K.; Ryu, M.; Kim, K.; Lee, S. *Macromolecules* **1998**, *31*, 1114.
(16) Zyung, T.; Hwang, D.; Kang, I.; Shim, H.; Hwang, W.; Kim, J. *Chem. Mater.* **1995**, *7*, 1499.
(17) Hu, B.; Karasz, F. E.; Morton, D. C.; Sokolik, I.; Yang, Z. *J. Luminescence* **1994**, *60−61*, 919.
(18) Li, X.; Cacialli, F.; Cervini, R.; Holmes, A. B.; Moratti, S. C.; Grimsdale, A. C.; Friend, R. H. *Synth. Met.* **1997**, *84*, 159.
(19) Onoda, M.; MacDiarmid, A. G. *Synth. Met.* **1997**, *91*, 307.

10.1021/cm000379o CCC: $19.00
Published on Web 08/12/2000

An analogous concept is to replace the sulfur atom in poly(nonylbithiazole) (PNBTz)[20] with oxygen leading poly(nonylbisoxazole) (PNBO) (shown below). This atomic change might cause more dramatic effects than the switch from carbon to nitrogen because both C and N are adjacent elements in the same row of the periodic table. Hence, the C−N and C−C overlap integrals are similar, as are the C−C and C−N bond distances. However, oxygen and sulfur are in adjacent rows of the periodic table and have quite different electronegativities, covalent radii, polarizabilities, and atomic orbital overlaps; factors which could lead to appreciable changes in intermolecular interactions in addition to changes in the molecular electronic structure. This paper reports our synthesis and characterization of a new conjugated polymer, poly(4,4′-dinonyl-2,2′-bisoxazole-5,5′-diyl) (PNBO). The physical and chemical properties of PNBO are compared with analogous heterocyclic polymers, poly(4,4′-dinonyl-2,2′-bithiazole-5,5′-diyl) (PNBTz) and poly(3-alkylthiophenes), P3ATs.

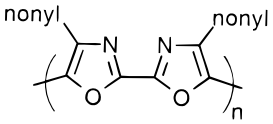

PNBO

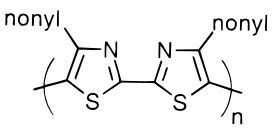

PNBTz

Experimental Section

All manipulations and polymerizations were performed under a nitrogen atmosphere using standard Schlenk line techniques unless otherwise stated. Reagents were purchased and used as received unless otherwise stated. ^{1}H NMR spectra were collected on a Bruker AM-360, AM-300, or AM-200 and referenced to the residual proton solvent resonance. UV−vis spectra were collected on a Shimadzu 3101PC with baseline correction. Emission spectra were collected on a Shimadzu 4121 interfaced with a Gateway computer. X-ray diffraction data were obtained on a Rigaku Rotaflex diffractometer operated at 40 kV, 100 mA equipped with a Cu target (λ = 0.154 nm) and a graphite monochromator. Samples were scanned from 3° to 35° (2θ) at 0.01° intervals and a rate of 1° per minute. The differential scanning calorimetry (DSC) and TGA were performed on a Perken-Elmer DSC 7 with 5−15 mg of powdered sample at scan rates of 10 °C/min unless noted otherwise. Elemental analyses were performed by either Galbraith Laboratories or the University of Michigan Microanalysis Laboratory. Cyclic voltammetry was performed with a three-electrode potentiostat designed and built by Wayne Burkhardt (University of Michigan, Department of Chemistry Electronics Shop) interfaced with a PC running a custom software program written by Dr. Steven Parus (University of Michigan, Department of Chemistry). The computer drives the voltage ramp and collects the current−voltage data. The electrolyte was 0.1 M tetrabutylammonium tetrafluoroborate in acetonitrile, the working and auxiliary electrodes were platinum, and the reference electrode was Ag/$AgNO_3$ in acetonitrile. Potentials are reported vs the potential of the ferrocene/ferrocinium couple obtained by adding a crystal of ferrocene to the solution at the conclusion of the experiment.

Synthesis of 5,5′-Dibromo-4,4′-dinonyl-2,2′-bisoxazole (Br_2-NBO). A 250-mL Schlenk flask equipped with an addition funnel, stir bar, and N_2 inlet/outlet was charged with nonylbisoxazole, NBO,[24] (3.12 g, 8.03 mmol) in CCl_4 (80 mL). The solution was cooled to 0 ° C, wrapped in Al foil, and bromine (2.82 g, 17.7 mmol) in CCl_4 (25 mL) was added dropwise over 15 min. The reaction was allowed to stir at room-temperature overnight. The solution was washed with aqueous sodium bisulfite (2 × 100 mL), aqueous potassium carbonate (2 × 50 mL), and H_2O (2 × 100 mL) and dried over $MgSO_4$. The solvent was removed under vacuum to give a yellow oil which solidified upon standing. The solid was recrystallized three times from acetonitrile to give white needles of Br_2−NBO. Yield = 2.85 g (64. 9%). ^{1}H NMR ($CDCl_3$): δ 0.88 (6H, t, J = 6.4 Hz, $-CH_3$), 1.15−1.45 (24H, m, $-(CH_2)_6CH_3$), 1.68 (4H, m, J = 7.1 Hz, ring-CH_2CH_2), 2.53 (4H, t, J = 7.5 Hz, ring-CH_2). Anal.: Calcd for $C_{24}H_{38}Br_2N_2O_2$: C, 52.75; H, 7.02; N, 5.13. Found: C, 52.78; H, 6.91; N, 5.12.

Synthesis of Poly(4,4′-dinonyl-2,2′-bisoxazole-5,5′-diyl) (PNBO). A dry, 100-mL Schlenk flask equipped with a stir bar and N_2 inlet/outlet was charged with Br_2−NBO (1.65 g, 3.02 mmol), Ni(COD)$_2$ (1.11 g, 3.93 mmol), and 2,2′-bipyridyl (0.66 g, 4.23 mmol) in dry xylenes (60 mL). A condenser was placed on the flask, and the reaction mixture was heated to reflux overnight. The dark, viscous mixture was precipitated by addition to a flask containing concentrated HCl (48 mL) in MeOH (352 mL), ∼5% HCl in MeOH. The dark orange solid was collected and extracted with hot xylenes (1 L). The solution was filtered, and the solvent volume was reduced to 50 mL. The solution was then added to 5% HCl in MeOH (400 mL). The yellow-orange precipitate was collected and dried under vacuum (fraction 1). The solid that did not dissolve in xylenes was dissolved in hot tetrachloroethane (1 L), and the solution was filtered. The solvent volume was reduced to 50 mL and added to 5% HCl in MeOH (400 mL). The orange precipitate was collected and redissolved in hot tetrachloroethane (500 mL). The solution was filtered, and the solvent volume was reduced to 50 mL. The polymer was precipitated into 5% HCl in MeOH (400 mL), collected by filtration, and dried under vacuum (fraction 2). Fraction 2 was used in the analysis. Anal.: Calcd for $C_{24}H_{38}N_2O_2$: C, 74.55; H, 9.93; N, 7.25. Found: C, 74.38; H, 9.71; N, 7.00. λ_{max} (abs) = 446, 465 nm ($C_2H_2Cl_4$); 475 nm (film). λ_{max} (em) = 528 nm ($C_2H_2Cl_4$); 540 nm (film). The GPC trace could not be obtained due the insolubility of the polymer in the GPC solvent, $CHCl_3$.

Results and Discussion

Preparation. Scheme 1 shows the overall synthesis of poly(4,4′-dinonyl-2,2′-bisoxazole-5,5′-diyl) (PNBO). PNBO was synthesized from 5,5′-dibromo-4,4′-dinonyl-2,2′-bisoxazole (Br_2−NBO) by coupling with Ni(COD)$_2$.[25]

(20) Nanos, J. I.; Kampf, J. W.; Curtis, M. D.; Gonzalez, L.; Martin, D. C. *Chem. Mater.* **1995**, *7*, 2232.
(21) Politis, J. K.; Curtis, M. D.; González, L.; Martin, D. C.; He, Y.; Kanicki, J. *Chem. Mater.* **1998**, *10*, 1713.
(22) Yamamoto, T.; Suganuma, H.; Maruyama, T.; Inoue, T.; Muramatsu, Y.; Arai, M.; Komarudin, D.; Ooba, N.; Tomaru, S.; Sasaki, S.; Kubota, K. *Chem. Mater.* **1997**, *9*, 1217.
(23) Curtis, M. D.; Cheng, H. T.; Nanos, J. I.; Nazri, G. A. *Macromolecules* **1998**, *31*, 205.
(24) Politis, J. K.; Somoza, F. V.; Kampf, J. W.; Curtis, M. D.; González-Ronda, L.; Martin, D. C. *Chem. Mater.* **1999**, *11*, 2274.

Scheme 1

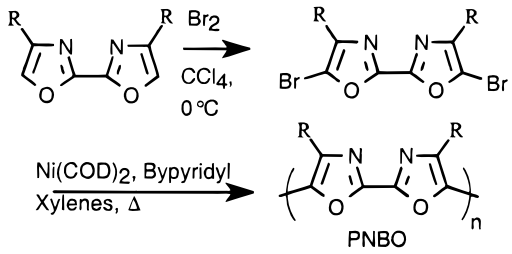

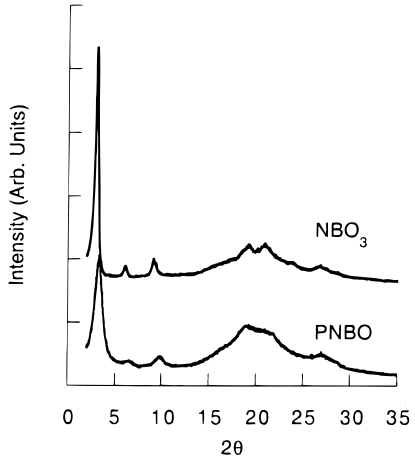

Figure 1. Powder X-ray diffraction patterns for PNBO and NBO-3.

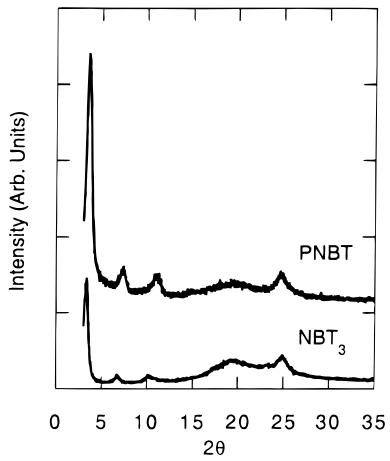

Figure 2. Powder X-ray diffraction patterns for PNBTz and NBTz-3.

The Br_2−NBO was prepared by direct bromination of NBO at 0 °C in CCl_4. The synthesis of NBO and its oligomers have been reported previously.[24] PNBO is less soluble in common organic solvents than either comparable P3ATs or PNBTz.

X-ray Data. Figure 1 presents the XRD powder patterns of PNBO with the trimer of NBO (NBO-3) and Figure 2 compares the XRD powder patterns of PNBTz with the trimer of NBTz (NBTz-3). Table 1 lists the reflections observed for each compound. The *d* spacings corresponding to the 100 reflection for PNBO, NBO-3, PNBTz, and NBTz-3 are 26.6, 29.2, 24.4, and 26.6 Å, respectively. The (100) reflection arises from the lamellar packing (lateral chain backbone to backbone distance).[26] The polymers exhibit a smaller d_{100} spacing than the trimers in both systems, and the oxazoles have a larger d_{100} than the thiazoles. It is uncertain what causes the decrease in lamellar distance in the polymers compared to the trimers, but side chain disorder resulting in nonfully extended alkyl chain conformations may be responsible. However, the larger lamellar spacings of PNBO and NBO-3 vs PNBTz and NBTz-3, respectively, may be explained by a molecular structure in which the alkyl groups in PNBO and NBO-3 lie in the plane of the rings, whereas in PNBTz and NBTz-3, the alkyl groups make an angle with respect to the plane of the rings. As shown in Scheme 2, the more planar molecule has a larger projection perpendicular to the chain axis, hence a larger lamellar spacing. The single-crystal structures of NBO[24] and NBTz[20] give support to this explanation. In NBO, the side chains lie in the plane of the rings, whereas in NBTz the torsion angle between the plane of the rings and projection of the nonyl side chain is 28° as shown in Scheme 2.

PNBO also has a peak at 27° corresponding to *d* spacing of 3.30 Å which may be identified with an interchain, π-stacking distance. Similar reflections are observed for NBO-3, PNBTz, and NBTz-3 which have *d* spacings of 3.33, 3.59, and 3.57 Å, respectively. Thus, in both the oxazole and thiazole series, the corresponding trimer−polymer pair have nearly identical π-stacking distances (d_{020}). However, the thiazoles have larger

Table 1. XRD Reflections for NBO-3, PNBO, NBTz-3, and PNBTz.

polymer	2θ (deg)	*d* spacing (Å)
	NBO-3	
lamellar spacing	3.0	29.2
	6.1	14.5
	9.1	9.7
interchain spacing	26.7	3.3
	PNBO	
lamellar spacing	3.3	26.6
	6.6	13.3
	10.0	8.9
interchain stacking	27.0	3.3
	NBTz-3	
lamellar spacing	3.3	26.6
	6.6	13.3
	10.2	8.7
interchain stacking	24.8	3.6
	PNBTz	
lamellar spacing	3.6	24.4
	7.2	12.2
	10.9	8.1
interchain stacking	24.8	3.6

Scheme 2

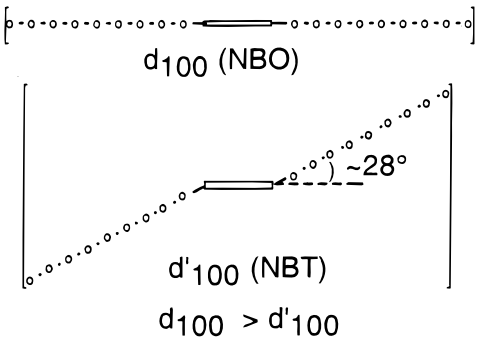

(25) Yamamoto, T.; Morita, A.; Miyazaki, Y.; Maruyama, T.; Wakayama, H.; Zhou, Z.; Nakamura, Y.; Kanbara, T.; Sasaki, S.; Kubota, K. *Macromolecules* **1992**, *25*, 1214.

(26) González-Ronda, L.; Martin, D. C.; Nanos, J. I.; Politis, J. K.; Curtis, M. D. *Macromolecules* **1999**, *32*, 4558.

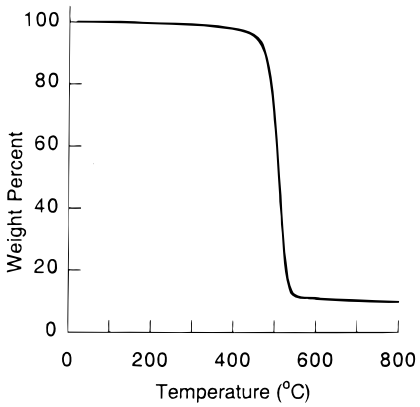

Figure 3. TGA of PNBO in a nitrogen atmosphere, powder sample, 20 °C/min.

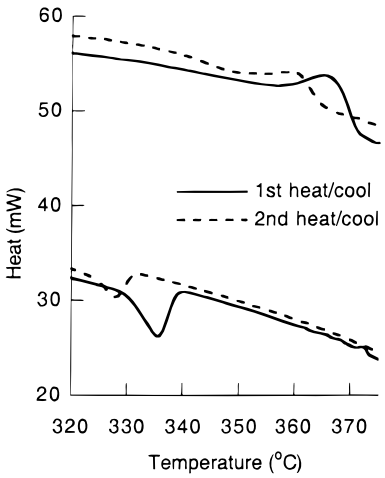

Figure 4. DSC traces of PNBO, first and second heat/cool cycles, powder sample at 20 °C/min.

π-stacking distances than the oxazoles. The larger stacking distance in the thiazoles may be related to the larger van der Waals radius of sulfur as compared to oxygen. This argument is weakened by the observation that HT regioregular poly(3-octylfuran) and poly(3-octylthiophene) have nearly identical π-stacking distances (3.81 and 3.79 Å, respectively), both of which are larger than the d_{020} spacing in PNBTz or PNBO.[27] Thus, other factors, such as the efficiency of side chain packing, must influence the π-stacking distance.

The similarities in the XRD patterns of PNBO with PNBTz and NBO-3 with NBTz-3 indicate the replacement of oxygen with sulfur does not effect the overall solid-state morphology of the polymers, and their solid state morphology is resistant to the effects of changes in bond lengths and electronics within the conjugated system caused by these atomic alterations. Also, the similarity between the XRD patterns of NBO-3 with PNBO and NBTz-3 with PNBTz clearly illustrates that the solid-state morphology of the polymers is essentially identical to that of the trimers (six rings). Hence, small oligomers can be used as models for determining the packing of a corresponding polymer in the solid state. The use of oligomers to model the spectra and structures of corresponding polymers is now well established.[28,29] We are currently attempting to grow diffraction grade crystals of the trimers.

An estimate of the degree of crystallinty as derived from the X-ray data of PNBO has not been attempted because we are unable to deconvolute the amorphous halo from the unresolved Bragg diffractions in the region $15° < 2\theta < 25°$.

Thermal Analysis. Figure 3 is a TGA plot of PNBO conducted under N_2. PNBO exhibits an onset of thermal decomposition, as determined by a 5% weight loss, at 452 °C ($T_{5\%}$). This is comparable to the corresponding $T_{5\%}$ for PNBTz, 480 °C.[20] DSC traces of the first and second heating cycles for PNBO are shown in Figure 4. On the first heating/cooling cycle, a melting endotherm at 366 °C and a crystallization exotherm at 335 °C are recorded. On the second heat/cool cycle, the melt occurs at 360 °C and crystallization at 327 °C. No other transitions were observed. PNBTz exhibits similar behavior with a melt transition at 305 °C during the first heating cycle.[26] The higher melting temperature of PNBO compared to that of PNBTz suggests that more energy is needed to disrupt the crystalline structure of PNBO. This would be consistent with the shorter π-stacking distance observed for PNBO by XRD, and is borne out by an analysis of the DSC data as shown below.

Table 2. Melting Temperatures and Normalized Heats of Fusion of NBO and NBTz Oligomers and Polymers

	n =			
	1	2	3	polymer
T_m (NBO-*n*), °C	81	128	172	365
T_m (NBTz-*n*), °C[a]	59	46 95	126	305
ΔH (NBO-*n*), kJ/NBO	60	20	19	5
ΔH (NBTz-*n*), kJ/NBTz[a,b]	48	11 23	14	14[c]

[a] There are two endotherms at the indicated temperatures with the corresponding ΔH values. [b] ΔH values are normalized to one bis(oxazole) or bithiazole repeat unit. [c] The value for PNBTz is an average from refs 24 and 26.

Table 2 lists the melting temperatures and values of the heats of fusion, ΔH_m, of NBO and NBTz oligomers and the polymers, PNBO and PNBTz, as measured by DSC.[24,26] The heats of fusion are normalized to the 2-ring, bisoxazole or bithiazole repeat unit. The melting temperatures, T_m, of both series, NBO-*n* and NBTz-*n*, increase monotonically as the chain length increases, culminating in the T_m of the respective polymers. The bithiazole dimer, NBTz-2, shows more complex behavior: two endotherms are observed at 46 and 95 °C. The corresponding exotherms on the cooling cycle occur at 69 and 23 °C, respectively. This behavior was reproducible through at least three heat/cool cycles. We attribute this behavior to the formation of a liquid crystalline phase between 46 °C and the clearing temperature of 95 °C. A future paper will report on the liquid crystalline behavior of NBTz-2 in more detail.

As expected from the higher melting temperatures, the oxazole oligomers have larger heats of fusion, ΔH_m, compared to the corresponding thiazoles. The monomer, 4,4′-dinonyl-2,2′-bisoxazole (NBO) has the largest heat of fusion, 60 kJ/mol. The dimer and trimer, NBO-2 and NBO-3, each have ΔH_m of 20 kJ/NBO-group. In the bithiazole (NBTz) series, the monomer has a ΔH_m of 48 kJ/mol. The dimer absorbs 11 and 23 kJ/NBTz, respec-

(27) Politis, J. K.; Curtis, M. D.; Nemes, J. C., submitted for publication.
(28) Tour, J. M. *Trends Polym. Sci.* **1994**, *2*, 332.
(29) Müllen, K.; Wegner, G. *Electronic Materials: the Oligomer Approach*; Wiley-VCH: New York, 1998.

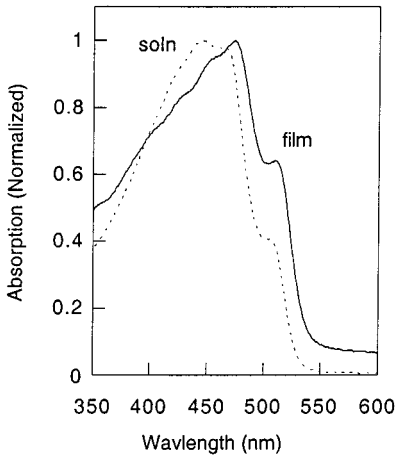

Figure 5. UV−vis spectra of PNBO solution and film.

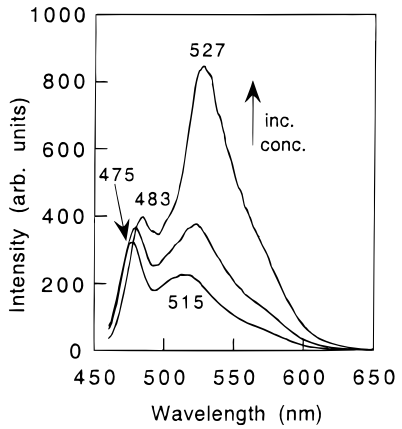

Figure 6. Emission spectra of solutions of different concentrations of PNBO excited at 446 nm.

tively, at its two endotherms. Thus, to go from the crystal to the isotropic liquid requires the sum, 34 kJ/NBTz. The ΔH_m of the trimer, 14 kJ/NBTz, is lower than that of the dimer but is the same as that of the polymer, PNBTz.

If one assumes the normalized heat of melting of the crystalline regions remains constant from the trimer to the polymer, then the ratio of the values of ΔH_m of the polymer and trimer may be used to calculate the degree of crystallinity in the polymer film. For PNBO, this ratio is 5/19 = 26%, and for PNBTz the ratio is 100%. The degree of crystallinity estimated from the XRD of PNBTz ranges up to 75%,[26] in reasonably good agreement with the estimate from DSC. The spectral data discussed below also support a lower degree of crystallinity in PNBO films, but a higher degree of aggregation in solution, as compared to PNBTz.

Spectral Data. Figure 5 plots the UV−vis spectra of PNBO in solution and as a spin-cast film. The solution spectrum has two intense peaks at 446 and 465 nm, and a shoulder at 507 nm. The film shows discernible shoulders at 403, 430, and 454, with λ_{max} = 475 nm, and a long wavelength shoulder at 510 nm. For the solid, the wavelengths correspond to frequencies of 24810, 23260, 22030, 21050, and 19760 cm^{-1}, respectively. The energy differences between adjacent shoulders are 1550, 1230, 980, and 1290 cm^{-1}. These frequencies are within the range of in-plane ring vibrations that contain components of C=C and C=N stretching modes. The corresponding frequencies and frequency differences found in the solution spectrum are 22400, 21500, and 19720 with $\Delta\nu$ = 900 and 1780 cm^{-1}. The 1780 cm^{-1} difference between the long wavelength shoulder and the absorption maximum is too large to be ascribed to any symmetric ring stretching modes, all of which are below about 1650 cm^{-1}.[30]

Yamamoto et al. have shown conclusively that the progression of peaks or shoulders in the spectra of regioregular polymers are associated with aggregate formation (π-stacking).[31] The spectra of nonaggregated solutions of regioregular P3ATs, PABTz's,[20,24] and poly(alkylfuran)s[27] (P3AFs) all consist of a single, relatively narrow, absorption peak. In the solid state, or in colloidal aggregates, there is a large bathochromic shift of λ_{max}, and typical "fine structure", i.e., a series of shoulders, also becomes evident. The shift of λ_{max} to long wavelengths is associated with an increase in the average conjugation length due to planarization of the polymer backbone in the π-stacked aggregates or crystalline regions of the solid. The cause of the fine structure is less settled. Some authors have attributed the shoulders to differing, yet distinct, conjugation lengths,[32] to vibronic coupling,[33] to Davydov splitting (inequivalent sites) in the solid,[34] and to a combination of Davydov splitting and exciton band structure.[35] The latter can produce broad absorptions centered around vibronic peaks, as well as additional structure caused by translationally inequivalent site effects.[35,36]

The emission spectra also show features associated with aggregate formation. Figure 6 shows the emission spectra for PNBO in solution at different concentrations. The appearance of the solution spectra depends greatly on the concentration of polymer. In dilute solution

(30) (a) Bellamy, L. J. *The Infrared Spectra of Complex Molecules*; John Wiley & Sons: New York, 1958. (b) Blanda, W. M.; Francis, A. H.; Curtis, M. D. Unpublished results.

(31) Yamamoto, T.; Komarudin, D.; Arai, M.; Lee, B. L.; Suganuma, H.; Asakawa, N.; Inoue, Y.; Kubota, K.; Sasaki, S.; Fukuda, T.; Matsuda, H. *J. Am. Chem. Soc.* **1998**, *120*, 2047.

(32) (a) McCullough, R. D.; Ewbank, P. C. In *Handbook of Conducting Polymers*; Skotheim, T. A., Elsenbaumer, R. L., Reynolds, J. R., Eds.; Mercel Dekker: New York, 1998; pp 243−247. (b) Chen, T.; Wu, X.; Rieke, R. D. *J. Am. Chem. Soc.* **1995**, *117*, 233.

(33) (a) Sakurai, K.; Tachibana, H.; Shiga, N.; Terakura, C.; Matsumoto, M.; Tokura, Y. *Phys. Rev. B* **1997**, *56*, 9552. (b) Danno, T.; Kuerti, J.; Kuzmany, H. *Front. Polym. Res., [Proc. Int. Conf.], 1st*; Prasad, P. N., Nigam, J. K., Eds.; Plenum: New York, NY, 1991; pp 219−222. (c) Yamamato, T.; Honda, K.; Ooba, N.; Tomaro, S. *Macromolecules* **1998**, *31*, 7. (d) Sandstedt, C. A.; Rieke, R. D.; Eckhardt, C. J. *Chem. Mater.* **1995**, *7*, 1057.

(34) (a) Halkyard, C. E.; Rampey, M. E.; Kloppenburg, L.; Studer-Martinez, S. L.; Bunz, U. H. F. *Macromolecules* **1998**, *31*, 8655. (b) Spano, F. C.; Siddiqui, S. *Chem. Phys. Lett.* **1999**, *314*, 481. (c) DiCésare, N.; Belletête, M.; Leclerc, M.; Durocher, G. *Chem. Phys. Lett.* **1998**, *291*, 487. (d) Chen, L. H.; Geiger, C.; Perlstein, J.; Whitten, D. G. *J. Phys. Chem. B* **1999**, *103*, 9161. (e) Langeveld-Voss, B. M. W.; Janssen, R. A. J.; Christiaans, M. P. T.; Meskers, S. C. J.; Dekkers, H. P. J. M.; Meijer, E. W. *J. Am. Chem. Soc.* **1996**, *118*, 4908. (f) Langeveld-Voss, B. M. W.; Waterval, R. J. M.; Janssen, R. A. J.; Meijer, E. W. *Macromolecules* **1999**, *32*, 227.

(35) (a) Koren, A.; Curtis, M. D.; Kampf, J. W. *Chem. Mater.* **2000**, *12*, 1519. (b) Curtis, M. D.; Blanda, W.; Politis, J. K.; Francis, A. H.; Lee, J.; Koren, A.; Kampf, J. W.; Gonzalez-Ronda, L.; Martin, D. C. *Mater. Res. Soc. Symp. Proc.* **1999**, *548*, 285.

(36) (a) Pope, M.; Swenberg, C. E. *Electronic Processes in Organic Crystals and Polymers*, 2nd ed.; Oxford University Press: New York, 1999. (b) Giacintov, N. E.; Swenberg, C. E. In *Luminescence Spectroscopy*; Lumb, M. D., Ed.; Academic Press: New York, 1978; p 239ff. (c) Broude, V. L.; Rashba, E. I.; Sheka, E. F. *Spectroscopy of Molecular Excitons*; Springer Ser. Chem. Phys. 16; Goldanskii, V. I., Ed.; Springer-Verlag: New York, 1985.

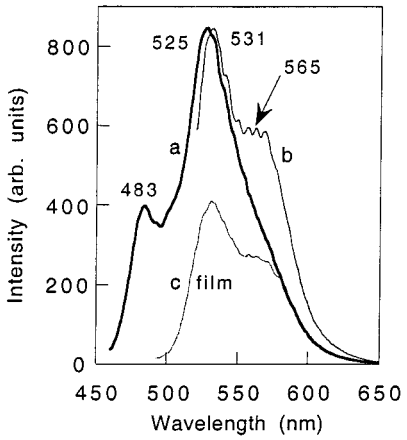

Figure 7. Emission spectra of a solution of PNBO excited at (a) 446 and (b) 506 nm, and (c) of a PNBO film excited at 446 nm.

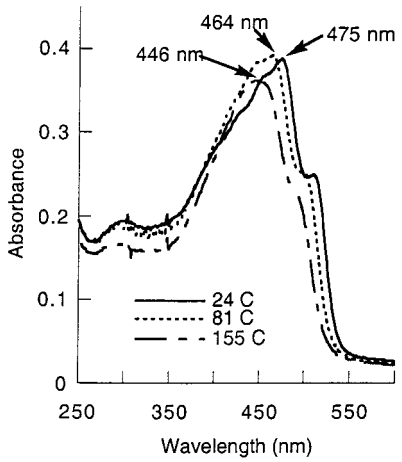

Figure 8. UV−vis spectra of a PNBO film at different temperatures.

(∼0.01 mg/mL), emission occurs at 475 and 515 nm when excited at 446 nm. There is also some emission at even longer wavelengths as shown by the gradual tailing off of the peak at longer wavelengths. At higher concentrations (<0.1 mg/mL), the long wavelength emission is enhanced relative to the 475 peak, whose position shifts slightly to 483 nm (a result of the larger contribution of the longer wavelength intensity to the overall peak profile). This behavior is consistent with the longer wavelength emission arising from excimers whose formation is favored by higher concentrations of chomophore.

Relaxation of the excited electronic state, S_1, to its lowest energy vibrational state is normally very fast compared to radiative decay to the ground state, S_0. Hence, the 0−0 transition is the highest energy transition in the emission spectrum, and it coincides with the lowest energy 0−0 absorption peak. The strong emission at 475 nm thus rules out the possibility that the peak at 510 nm is the 0−0 origin of the series of vibronic peaks observed in the solid or the solution absorption spectra. The 510 nm peak is thus assigned to a transition associated with aggregated species. The data shown in Figure 7 support this assignment. Compared to the emission spectra obtained with 446 nm excitation, there is enhanced emission at 565 nm when the solution is excited at 506 nm, i.e., 506-nm excitation favors emission from the low-energy excimer states. Formation of an excimer would be especially favorable if the molecules are already aggregated in the ground state. The emission spectrum of the solid film excited at 446 nm is nearly identical to the solution spectrum excited at 506 nm. The appearance of the solid-state emission spectrum is unchanged when the excitation wavelength is changed from 446 to 506 nm. This suggests that the transfer of excitation energy to low-energy aggregates is very efficient in the solid state, so that no matter what the excitation wavelength, all the emission occurs from excimers.

These conclusions are at slight variance with those reported in a recent paper by Bunz et al.[37] These authors report absorption and emission spectra of aggregated poly(phenylene-ethynylene)s (PPEs) that are strikingly similar to those exhibited here and elsewhere,[35] but Bunz et al. conclude that the low-energy shoulders in the absorption spectra can be adequately explained by a single-chain transition that becomes allowed as a result of the planarization of the main chain. Since the planarization is induced by aggregate formation, these authors describe the low energy shoulder as "aggregate induced" rather than an "aggregate absorption". The main basis for their conclusion is that the calculated energy shifts due to planarization (0.35 eV) are similar to the observed energy diference between λ_{max} and the low-energy shoulder. We have shown elsewhere that the exciton bandwidth due to π-stacking and the Davydov splitting also have a magnitudes around 0.3 eV.[35] Reference 24 contains further discussion of the relative effects of planarization vs aggregation.

Thermochromism. Figure 8 shows the UV−vis spectra of a spin coated PNBO film at different temperatures. At elevated temperatures, the absorption of PNBO blue shifts continually until the λ_{max} of the solution is reached. The shift is caused by thermal disorder that leads to twisting of the rings until the average conformation of the main chain approaches that found in the aggregates in solution. The relatively small shift from solution to solid (∼10 nm, vs 93 nm for PNBTz) shows that the structure in the solution aggregates is essentially identical to the solid-state structure. The same trend was observed in NBO and NBTz oligomers.[24]

A plot of $1/\lambda_{max}$ vs $1/n$ for NBO oligomer films gave a straight line ($1/\lambda_{max} = 1.83 \times 10^{-3} + 1.80 \times 10^{-3}/n$, $R = 0.9997$).[24] Hence, the absorption peaks at 465 and 475 nm corresponds to conjugation lengths of 5.6 and 6.5 repeat units (11 and 13 rings) for the solution and solid, respectively. PNBTz behaves somewhat differently than PNBO. In solution, PNBTz exhibits a featureless absorption with λ_{max} = 434 nm corresponding to ∼2.7 repeat units (5.4 rings). A spin-coated film of PNBTz shows an absorption spectrum essentially identical to that in solution. However, upon standing at room temperature, or upon thermal annealing, the amorphous, yellow film crystallizes and turns red. In the UV−vis spectrum, an isosbestic point is observed as a new absorption grows in at 527 nm while the 434 nm absorption decreases in intensity. As in solution, the

(37) Miteva, T.; Palmer, L.; Kloppenburg, L.; Neher, D.; Bunz, U. H. F. *Macromolecules* **2000**, *33*, 652.

conjugation length in the yellow, amorphous phase is 2.7 repeat units in length, whereas in the crystalline phase, the chromophore is extended to 34 repeat units (68 rings), as calculated from extrapolation of the linear plot of $1/\lambda$ vs $1/n$.[20]

The different behavior of PNBO is attributed to its more polar character, lower solubility, and aggregated state in solution as compared with PNBTz. The small aggregates of PNBO remain more or less intact as solvent is removed during film formation, whereas rapidly solidified films of PNBTz are initially disordered because the randomly oriented chains in solution are tangled together during solvent evaporation. The chains in the disordered state are capable of sufficient movement to crystallize, but are then immobilized in the crystalline phase. With PNBO on the other hand, the crystallite size and structure are mostly determined by the size and structure of the aggregates in *solution* because the molecules in the aggregates are already immobilized in the aggregates as the film is being cast. Thus, the crystallite size and order of PNBO films do not increase upon annealing or standing as do films of PNBTz; and, although more aggregated in solution, the degree of crystallinity of PNBO films is less than that of PNBTz films as measured by DSC.

Holdcroft has shown that the thermochromic behavior of P3ATs is related to the regioregularity and length of the side chains.[38] Regioregular P3ATs with short alkyl side chains, show a gradual blue shift in λ_{max} as the temperature is increased. In contrast, polymers with longer alkyl side chains show an abrupt order−disorder transition marked by an isosbestic point in the spectrum. This work shows that the nature of the main chain also influences greatly the thermal behavior of poly(alkylheteroarenes). Increasing the polarity of the main chain increases the rigidity of the lattice, and longer alkyl side chains are required to restore sufficient flexibility to the lattice for the order−disorder transition to occur. Apparently, nonyl side chains are not long enough to "plasticize" the lattice, and the UV−vis spectrua are not affected appreciably by heating to 155 °C. Instrumental limitations prevented us from heating the sample to higher temperatures, but we believe PNBO would show more pronounced changes near its melting temperature, 365 °C.

Cyclic Voltammetry. Figure 9 displays the CV curve of a film of PNBO on a Pt working electrode. The curve shows two reduction waves at −2.11 and −2.49 V (vs the Fc/Fc^+ couple referenced to $E = 0.00$ V). A two-peaked reduction wave is typical of electroactive polymers in which there is a relatively strong coupling between reducible centers.[39] The first peak roughly corresponds to the reduction of every other bis(oxazole) group; the second wave corresponds to the reduction of the remaining groups that are surrounded by groups that are already reduced. The reduction appears to be irreversible, but rescanning the negative potential region reveals that the polymer film had detached from the electrode surface upon reduction. We were unable to find a combination of solvent and electrode surface which allowed the oxidized or reduced polymer to adhere to the electrode surface. The reduction of bis(oxazole) oligomers in solution is reversible,[24] so there is no reason to believe the reduction of the polymer would not be chemically reversible. The oligomers show one reduction peak per bis(oxazole) group. A weak oxidation peak is seen on the reverse scan near 1.19 V. The weakness of the peak results from the detachment of the film. A strong current is observed if the sweep is first taken to positive potentials. For comparison, PNBTz is reduced near −1.98 V,[23] and is irreversibly oxidized near 1.2 V. Poly(alkylthiophene)s are oxidized near +0.6 V.[40] Thus, n-doped PNBO is unstable toward oxygen or water environment, and the high oxidation potential renders p-doping impractical.

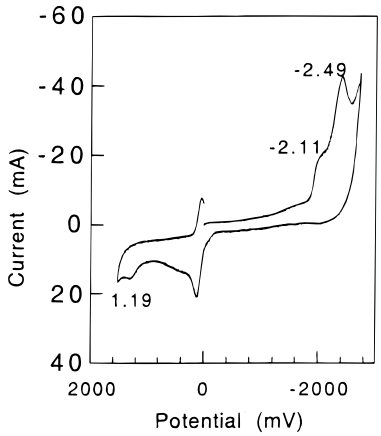

Figure 9. CV curve of PNBO film on a Pt working electrode, sweep rate = 500 mV/s.

Conclusions

Poly(4,4′-dinonyl-2,2′-bisoxazole-5,5′-diyl) (PNBO), the first member of a new class of conjugated polymers, has been prepared. Poly(alkylbisoxazole)s (PABOs) are related to poly(alkylbithiazoles) (PABTz's) by replacement of sulfur by oxygen. The solid-state morphology and thermochromic properties of PNBTz and PNBO are similar to those of more familiar, regioregular poly(3-alkylthiophenes), P3ATs. However, significant differences exist: PNBO is aggregated in solution (even in the best solvent found) such that solution absorption and emission spectra resemble those of the solid state. The strong aggregation is also reflected in the thermochromic behavior: PNBTz shows an order−disorder transition in the solid state, whereas PNBO does not. It appears that the detailed behavior of order−disorder transitions, thermochromism, and solid-state morphology results from a subtle balance of forces between the alkyl side chains and the main chains, and the latter interactions depend heavily on polarity and the polarizability of the heteroaromatic rings.

Acknowledgment. The authors thank the National Science Foundation (DMR-9510274) for support for this research. We especially thank Mr. Joel Nemes for performing the CV experiments, and Mr. Mathew Brukwicki for measuring the ΔH_m of the NBTz oligomers.

CM000379O

(38) Yang, C.; Orfino, F. P.; Holdcroft, S. *J. Am. Chem. Soc.* **1996**, *29*, 6510.

(39) Aoki, K.; Chen, J. *J. Electroanal. Chem.* **1995**, *380*, 35.

(40) McCullough, R. D.; Tristram-Nagle, S.; Williams, S. P.; Lowe, R. D.; Jayaraman, M. *J. Am. Chem. Soc.* **1993**, *115*, 4910.